Slow neural oscillations explain temporal fluctuations in distractibility

Troby Ka-Yan Lui, Jonas Obleser, & Malte Wöstmann

1. Department of Psychology, University of Lübeck, Ratzeburger Allee 160, 23562 Lübeck, Germany
2. Center of Brain, Behavior and Metabolism, University of Lübeck, Ratzeburger Allee 160, 23562 Lübeck, Germany

Corresponding author

Malte Wöstmann (malte.woestmann@uni-luebeck.de)

Acknowledgments

This research was supported by funding from the Deutsche Forschungsgemeinschaft (DFG; grant number: WO 2371/1-1) awarded to MW. We thank Frauke Kraus and Malte Naujokat for their help in data collection.

Competing interests

The authors declare no conflict of interest.

Data availability

Raw data are available from the corresponding authors upon request. Pre-processed behavioural and neural responses as a function of distractor onset time will be made available online upon publication.

Author contributions

Conceptualization, T.K.L., J.O., and M.W.; methodology, T.K.L., J.O., and M.W.; investigation, T.K.L. ; formal analysis, T.K.L., J.O., and M.W. ; writing – original draft, T.K.L. and M.W.; writing – review & editing T.K.L., J.O., and M.W.; funding acquisition, M.W.

Abstract

Human environments comprise various sources of distraction, which often occur unexpectedly in time. The proneness to distraction (i.e., distractibility) is posited to be independent of attentional sampling of targets, but its temporal dynamics and neurobiological basis are largely unknown. Brain oscillations in the theta band (3–8 Hz) have been associated with fluctuating neural excitability, which is hypothesised here to explain rhythmic modulation of distractibility. In a pitch discrimination task with unexpected auditory distractors (N = 30), we show that distractor-evoked neural responses in the electroencephalogram and perceptual susceptibility to distraction were co-modulated and cycled approximately 3–5 times per second. Pre-distractor neural phase in left inferior frontal and insular cortex regions explained fluctuating distractibility. Thus, human distractibility is not constant but fluctuates on a sub-second timescale. Furthermore, slow neural oscillations subserve the behavioural consequences of a hitherto largely unexplained but ever-increasing phenomenon in modern environments – distraction by unexpected sound.

Introduction

Selective attention enables humans to focus on relevant information at the expense of distraction. The brain prioritizes representations of relevant events while filtering out task-irrelevant distractors[1,2]. Recent research posited that distractor processing is not merely collateral to attentional sampling of targets but may follow its own dynamics[3–5]. The behavioural detriments induced by different kinds of distractors (i.e., *distraction*) and the neuro-cognitive mechanisms that counteract distraction (i.e., *suppression*) have been studied in some detail[4,6–9]. However, the temporal dynamics and the neurobiological basis of the proneness to distraction (i.e., *distractibility*) are largely unknown.

Distractibility has long been neglected in the theoretical formulation of rhythmic attention. Originally assumed to be static[10], the attentional spotlight was proposed to be blinking at a subsecond time scale in a theta-like rhythm (i.e., 3–8 Hz)[11,12]. Behaviourally, it is manifested via the waxing and waning of behavioural performance in target selection[13–16] or working memory[17,18] performance at similar frequencies. However, the temporal dynamics outside of the attentional spotlight are not well understood. While previous research studied how distractibility unfolds on relatively long temporal scales of minutes (i.e., during an experimental session[19]) or years (i.e., across stages of development[20,21]), we found preliminary evidence for fluctuating distractibility on a subsecond scale following rhythmic presentation of auditory targets[5]. To isolate distractibility dynamics from rhythmic entrainment or preparatory suppression, we here employ a design that uses non-rhythmic stimuli and distractors that occur unexpectedly.

A central prediction of rhythmic attention is that the phase of slow neural oscillations explains fluctuations in behaviour[22]. The prediction is based on the notion that rhythmic attention arises from the periodic excitability of the attention-related brain network[12,22]. In the human brain, theta neural phase (3–8 Hz) is assumed to reflect moment-to-moment changes in neural excitability[23]. Theta phase in brain regions beyond sensory cortices, such as fronto-parietal regions and the hippocampus, has been associated with fluctuations in target detection[24] and working memory encoding[25,26], respectively. While previous research has related distractibility to supra-modal regions in frontal[27,28] or parietal[29] cortex, it is unclear whether and in which networks the momentary neural dynamics may subserve the waxing and waning of distractibility.

Here, we ask if the brain spontaneously alternates between states of higher and lower distractibility and whether such fluctuations have the potency to explain behavioural consequences of distraction. If so, we would expect to observe a brain-behaviour relation between the pre-distractor brain state and the distractor-induced detriment in task performance. To this end, we employed a pitch discrimination task wherein an auditory distractor could occur at variable and unexpected times in-between two target tones. A total of 17,280 behavioural and neural responses in the electroencephalogram (EEG) in N=30 participants revealed that behavioural sensitivity and distractor-evoked neural responses fluctuated in sync across distractor onset times in ~3–5 cycles per second. Critically, pre-distractor theta phase in left inferior frontal and insular cortex regions explained behavioural performance fluctuations. These effects were absent in trials without distractors, reinforcing their specificity to distractor-related neural processing.

Results

In the current electroencephalography (EEG) and behavioural study, we aimed at (1) uncovering the temporal fluctuations in distraction, and (2) exploring the relationship between such fluctuations and momentary neural phase at similar frequencies. To this end, we varied the onset time of an auditory distractor that was presented in-between two to-be-compared tones in a variant of a pitch discrimination task.

We probed this research question in the auditory modality as temporal information is especially important to auditory attentional selection[30]. During the task, participants (N = 30) had to identify whether the two target tones were the same or different in pitch (Figure 1A). The distractor was a fast-varying, 25-Hz modulated sequence of tones that differed in pitch, which allowed us to extract its induced 25-Hz neural response[31].

Distractors were present in half of the trials and absent in the remaining trials. In distractor-present trials, the distractor onset was uniformly distributed across 24 onset times (0 – 1.15 s, in 0.05 s steps, after tone 1 offset). In distractor-absent trials, no distractor was presented between the two tones. The inclusion of distractor-absent trials serves two purposes. First, we could verify that the distractors had the potency to distract by comparing behavioural performance for distractor-present versus distractor-absent trials[32]. Second, participants could not anticipate whether or when a distractor would occur in a given trial, which eliminated potential effects of such anticipation on behavioural performance[33] or pre-stimulus neural activity[34–36].

Distractors interfere with pitch discrimination performance

To examine the potency of the distractors to distract, we compared participants' sensitivity and criterion (response bias) of the pitch discrimination task between distractor-present and -absent trials. Participants were less sensitive to the pitch difference (t_{29} = -8.11, p = <.001, Cohen's d = -1.48), and had a more conservative response criterion (i.e., more "same pitch" responses; t_{29} = 2.83, p = .008, Cohen's d = 0.52) on distractor-present trials (Figure 1B).

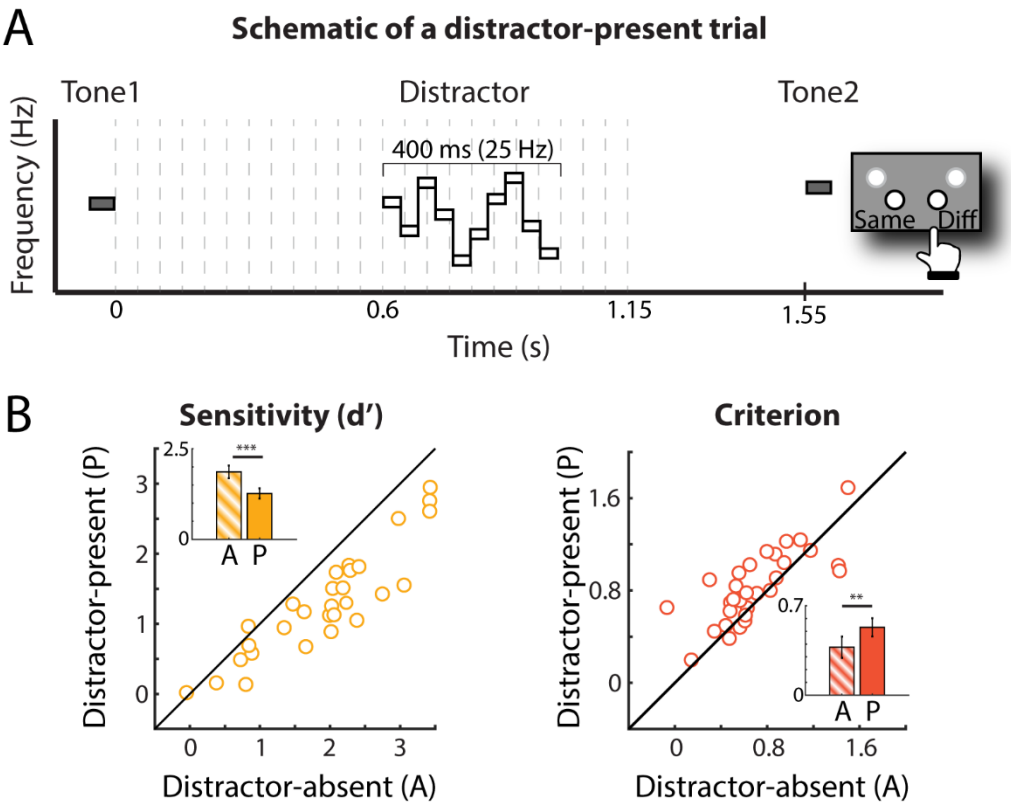

Figure 1. A) Schematic of a distractor-present trial. Participants were instructed to indicate whether the two target tones (grey) were the same (probability = 50%) or different (higher, probability = 25%; or lower, probability = 25%) in pitch. A 10-tone-pip distractor sequence (white) with a 25-Hz temporal structure (i.e., 40-ms tone-pip duration; total duration 400 ms) was presented at one of the 24 distractor onset times (dashed lines). In distractor-absent trials, no distractor was presented. B) Behavioural results comparing distractor-present and -absent conditions. Coloured circles indicate single-subject data. Insets show bar graphs of perceptual sensitivity (left panel) and criterion (right panel) for distractor-present (solid bar) and distractor-absent (gradient bar) conditions, respectively. Error bars show ±1 SEM. ** $p < .01$. *** $p < .001$.

Behavioural and neural measures of distraction co-fluctuate across time

Does the impact of distraction on neural activity and goal-directed behaviour exhibit fluctuations across time? To test this, we varied distractor onset time and examined whether behavioural and neural measures of distraction would show modulations at frequencies up to 8 Hz. Behaviourally, perceptual sensitivity was calculated as an indirect measure of distraction: The more distracted, the lower the sensitivity in pitch discrimination should be (Figure 2A, yellow, see Figure S1 for individual participants' time courses). Neurally, we calculated the distractor-evoked event-related potential (ERP; Figure 2B) for each distractor onset time and used a fast Fourier transform (FFT) to extract its amplitude at 25 Hz, which corresponded to the modulation rate of the frequency-modulated distractor tone sequence (Figure 2A, blue, see Figure S1 for individual participants' time courses).

To examine temporal fluctuations of distraction, we used linear mixed-effects models with sine- and cosine- transformed distractor onset time as predictors to model behavioural (i.e., perceptual sensitivity) and neural (i.e., distractor-evoked ERP) time courses as the outcome measures. This method outperforms other methods for studying the phasic modulation of behavioural and neural responses[37] and has also been used previously[5] to extract temporal fluctuations in the vulnerability of working memory to distraction. A quadratic trend was observed in the behavioural time course in Figure 2A as the earliest and latest distractors were most distracting due to their temporal proximity to the target tones. Before running linear mixed models, we removed the quadratic trends in the two measures as they were not of interest in the current study[38].

Figure 2E and F show the spectral magnitude (0.5–8 Hz, 0.5-Hz steps) resulting from linear mixed models on detrended perceptual sensitivity (Figure 2C, yellow) and detrended ERP amplitude (Figure 2C, blue), respectively. Statistical significance was derived by testing empirical spectral magnitude against the 95th percentile of a permutation distribution, which was derived from shuffling the behavioural and neural time courses, respectively, 5,000 times (see Methods for details).

At the behavioural level, distractor onset time modulated sensitivity below 5 Hz. At the neural level, distractor onset time modulated the distractor-evoked ERP at 4 and 5 Hz. Similar results were obtained in a control analysis, where temporal fluctuations in sensitivity in distractor-present trials were compared against distractor-absent trials (instead of permuted distractor-present trials; Figure S3).

If these periodic neural dynamics serve as the basis for the apparent behavioural fluctuations, we should observe the synchronization of the behavioural and neural time courses by a common rhythm. To test this, we also examined the co-modulation of sensitivity and distractor-evoked ERP by distractor onset time. We first calculated the cross-correlation coefficients of the behavioural and neural time courses for individual participants (Figure 2D). We then ran a linear mixed model with the cross-correlation coefficient as the outcome measure and sine- and cosine-transformed time lag as predictors.

Figure 2G shows that sensitivity and distractor-evoked ERP are co-modulated at 3.5 and 5 Hz. At lag 0, there was a negative correlation between sensitivity and the distractor-evoked ERP, consistent with the notion that stronger distractor encoding (i.e., larger distractor-evoked ERP) corresponds to worse task performance (i.e., lower sensitivity). T-tests against zero on the (Fisher-z transformed) correlation coefficients across participants show that this correlation at time lag 0 was close to statistical significance (Pearson's r: $t_{29} = -1.85$, $p = 0.08$, mean Pearson's $r = -0.08$; Spearman's r: $t_{29} = -2.13$, $p = 0.04$, mean Spearman's $r = -0.10$).

As a control analysis, the same analysis pipeline was run on the data in the distractor-absent condition by randomly assigning a "distractor onset" for each distractor-absent trial, which did not reveal any significant co-modulation (Figure S4): Neither time courses of sensitivity nor distractor-evoked ERP were modulated by distractor onset time; time lags did not modulate the cross-correlation of these two at any frequency. The temporal co-fluctuations of behavioural and neural measures of distraction at 3 – 5 Hz in distractor-present trials may be a manifestation of an underlying distractibility rhythm, which we probed into next.

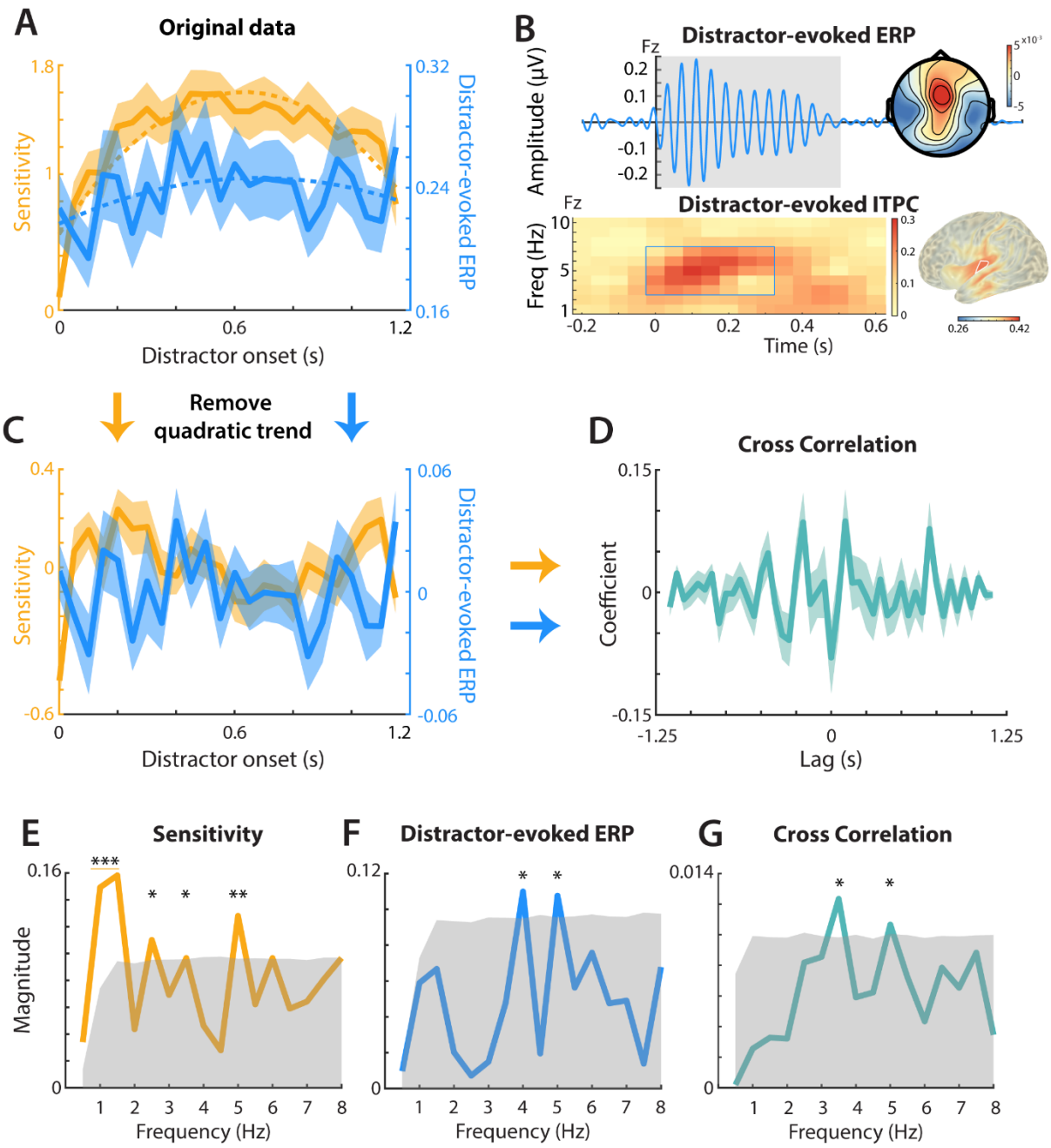

Figure 2. A) Average sensitivity (yellow solid line) and 25-Hz amplitude of the distractor-evoked event-related potential (ERP; blue solid line) across distractor onset times. Shaded areas show ±1 SEM across participants. Dashed lines show respective quadratic trends. B) Top panel: Distractor-evoked ERP waveform averaged across all distractor onset times at electrode Fz (20 – 30 Hz bandpass filtered for visualization purpose). Shaded grey area marks the time window used to extract the 25-Hz amplitude of the distractor-evoked ERP. Inset shows the scalp map of the 25-Hz amplitude of the distractor-evoked ERP (derived via an FFT on the distractor-evoked ERP waveform). Bottom panel: Distractor-evoked inter-trial phase coherence (ITPC) from 1 – 10 Hz and from -0.2 s – 0.6 s at Fz. Brain surface shows the ITPC values (frequencies: 3 – 7 Hz; time window: 0 – 0.3 s) in source space, which reflects the auditory response to the distractor. White outline indicates top 1% voxels with largest ITPC values. C) Detrended time courses of behavioural and neural outcome measures. Shaded areas show ±1 SEM across participants. D) Solid line shows average correlation coefficients, derived by averaging single-subject cross-correlations of sensitivity and distractor-evoked ERP time courses, as a function of temporal lags. Shaded area shows ±1 SEM across participants. E-G) Spectral magnitude across frequencies (0.5 – 8 Hz, 0.5-Hz step) for (E) detrended sensitivity, (F) distractor-evoked ERP, and (G) the cross-correlation between the two. Shaded areas show the 95th percentile of the permutation distribution generated from 5,000 permutations. * $p < .05$. ** $p < .01$. (uncorrected)

Pre-distractor neural phase in inferior frontal/insular cortex explains distraction

If the human brain hosts an endogenous rhythm that underlies distractibility dynamics, the neural state prior to distractor onset should explain the participant's momentary vulnerability to interference by a distractor. To test this, we studied how pre-distractor neural phase relates to our previously established proxy of distraction, that is, behavioural sensitivity. We asked when in time and in which brain network(s) such an endogenous rhythm underlying distractibility would show up.

We employed source-projected EEG time courses to extract the quadratic relationship between the binned pre-distractor neural phase and perceptual sensitivity. For each trial (Figure 3A), we first transformed a source-projected EEG data segment (0.4 s; sliding window) into the frequency domain using FFT. We then extracted neural phase for a given frequency (Figure 3B). To calculate sensitivity sorted by phase bin, we first sorted the trials according to their phase values into 9 phase bins of equal size, followed by calculation of perceptual sensitivity for each bin (see Figure S5 for individual participants' sensitivity by phase bin). The same procedure was repeated for a range of frequencies (2.5 – 8 Hz, 0.5-Hz steps) and time windows (-0.3 – 0.3 s around distractor onset, 0.05-s steps). A cluster-based permutation test with the dimensions time, frequency, and voxels, wherein the quadratic fit was tested against zero, revealed a positive significant cluster (Figure 3C; the same analyses with 7, 8, and 10 phase bins yielded comparable clusters across all dimensions and comparable statistical significance). The quadratic modulation of sensitivity by neural phase at 2.5 – 7.5 Hz was most prominent in the left insular and the inferior frontal cortices in the time window spanning ~300 ms before distractor onset (cluster p-value = .026, two-tailed; see Figure S6 for brain surface plots from other viewing angles).

To test whether the significant cluster overlaps with sources of auditory-evoked activity in auditory cortex regions, we compared its source with the source of distractor-evoked inter-trial phase coherence (ITPC) at 3 – 7 Hz (shown also in Figure 2B, bottom panel). Importantly, although the two effects were localized in proximal cortical regions (Figure 3C, bottom panel), their core regions were mostly non-overlapping.

For control, we conducted the same analysis on the distractor-absent trials, which revealed no significant cluster (Figure S7). We also tested the relationship between the pre-distractor neural phase and the post-distractor neural measure of distraction (i.e., 25-Hz amplitude of the distractor-evoked ERP), which did not reveal a significant effect (Figure S8).

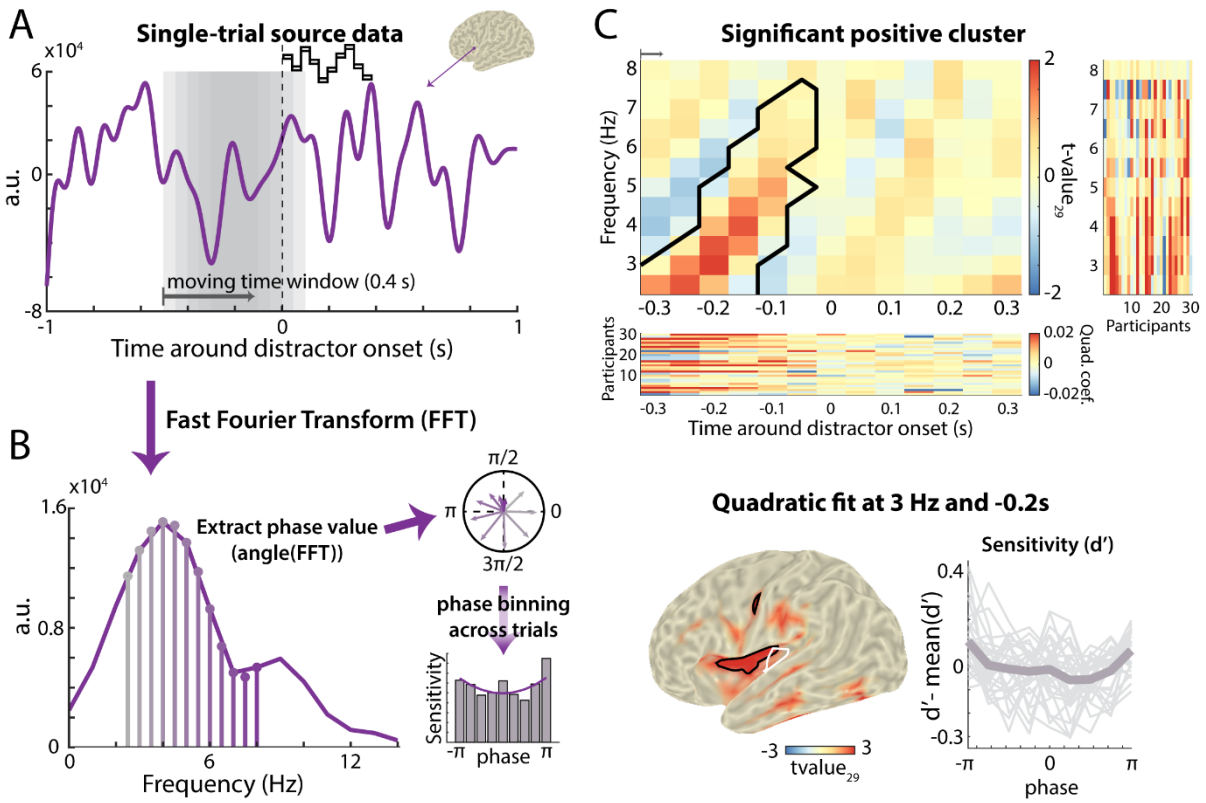

Figure 3. A-B) Illustration of the source-level analysis. A) Example of a single-trial source-projected EEG time course. The moving window (grey) was used to transform segments of the data into the frequency domain using FFT. The first grey window corresponds to the first time window used in the time-resolved analysis (i.e., -0.5 to -0.1 s). B) Spectral representation of the data segment in (A). Phase values across frequencies were extracted and trials were binned according to their phase values into 9 phase bins for each frequency, time window, and source location. Bar graph shows exemplary sensitivity values calculated from the trials sorted by phase bin. A quadratic trend was fitted to the sensitivity values across phase bins (purple solid line). C) Results of a cluster-based permutation test, which tested quadratic fits in time-frequency-source space against zero. Top panel shows the t-values (df = 29) across frequencies and time windows, averaged across all the voxels belonging to the significant positive cluster. The black contour indicates the positive significant cluster. Right column shows individual participants' quadratic coefficients for each frequency, collapsed across the time windows included in the significant cluster. Bottom row shows individual participants' quadratic coefficients across time windows, collapsed across frequencies and voxels included in the significant cluster. Bottom left panel shows the cluster peak effect (3 Hz; -0.2 s), which resides mainly in left inferior frontal cortex and insular cortex. Only the t-values of the positive significant cluster are shown. The black contour indicates the regions with the top 1% t-values across the whole brain. The t-values were interpolated and projected onto MNI coordinates for visualization purposes. The white contour indicates distractor-evoked neural activity, quantified as the top 1% inter-trial phase coherence (ITPC) in the post-distractor time window (i.e., 0 – 0.3 s) at 3 – 7 Hz (shown also in Figure 2B). Bottom right panel shows centred perceptual sensitivity sorted by phase bins in the positive cluster at 3 Hz averaged across participants. Grey thin lines show individual centred perceptual sensitivity.

Discussion

The current study aimed to unravel the temporal dynamics of distractibility, using a pitch discrimination task with auditory distractors. The eventual degree of distraction and the neural processing of distractors were respectively quantified by distractor-evoked performance detriments and neural responses in the human electroencephalogram (EEG). We made a series of interesting observations.

First, the ~3 – 5 Hz fluctuations of behavioural sensitivity across distractor onset time urged for the question whether the same fluctuations are observed in the human brain's response to distractors. Consistently, we found that the distractor-evoked neural response covaries with behavioural sensitivity at similar frequencies. Second, while behavioural sensitivity and the distractor-evoked neural response might partly reflect post-perceptual processes (such as distractor suppression), we asked whether the brain hosts an endogenous oscillation that shapes the momentary state of distractibility. Confirming this, we found that pre-distractor neural phase in left inferior frontal/insular cortex explained rhythmic fluctuations in the momentary degree of distraction.

These major findings support the notion that temporal fluctuations in distractibility on a subsecond time scale can be explained by slow neural oscillatory dynamics in a cortical network beyond the auditory cortex.

The proneness to distraction is inherently dynamic

The current study sheds light on the dynamics of distractibility, which is an important factor often neglected in previous attention research on distraction and suppression. The ultimate degree of detriment that a distractor will cause depends on two endogenous factors: the momentary proneness to distraction (i.e., distractibility) and the ability to suppress a distractor (i.e., distractor suppression). On the one hand, research on distractor suppression often did not disentangle the active suppression of distractors[39] from variations in distractibility. On the other hand, research on distractibility rather treated it as an individual characteristic that, if at all, only changes on a slow temporal scale such as within an experimental session[19] or across developmental stages[21]. The temporal trajectory of distractibility on a faster, subsecond, time scale had hitherto been left unknown.

With distractor-evoked behavioural and neural measures, we were able to encapsulate the temporal trajectory of distraction, which fluctuates on a subsecond temporal scale consistent with the rate of rhythmic sampling in attention[13–16] and working memory[17,18,40]. With analysis of pre-distractor neural oscillatory phase, we were able to trace this distractibility back to a slow neural oscillatory fluctuation in inferior frontal and insular cortex (see below for an in-depth discussion). Participants could not anticipate whether or when the distractor would occur, thereby not being able to engage in preparatory suppression of the upcoming distractor[41]. The combined analysis of pre-distractor neural phase and of post-distractor neural and behavioural measures complementarily elucidates how the brain alternates between states of higher and lower distractibility. These insights are essential for the inclusion of an explicit account of distraction in models of attention in psychology and neuroscience.

Fluctuations of distractibility at 3 – 5 Hz in the current study unveil the dynamic nature of attention, which was underappreciated in the static spotlight metaphor of attention[10]. The attentional sampling of to-be-attended external stimuli[13–15] or internal memory representation[17,18,40] has been shown to exhibit temporal fluctuations at similar frequencies. The waxing and waning of attentional sampling may index inter-areal coordination between the attentional network and the sensory areas of the brain[42], which is associated with the alternation between stronger and weaker attentional sampling over time[12]. With much evidence on the temporally dynamic nature of the attentional spotlight, however, there is a lack of theoretical foundation for the inherent dynamics of cognition outside of this spotlight[43]. With the observed fluctuations of distractibility in the theta frequency range, an extension of the existing theory of dynamic attentional sampling to temporally dynamic distraction is warranted.

While our results demonstrate that distractibility exhibits temporal fluctuations, they do not reveal whether such fluctuations are independent of the fluctuations found in the attentional sampling of memory content. Participants in the current study had to maintain the memory representation of the pitch of tone 1 during a trial. The theta fluctuations found in the current study thus may represent the sampling of the internal representation of tone 1, with higher distractibility hypothetically occurring during the phase of reduced sampling of the memory representation. Alternatively, observed theta fluctuations may represent independent fluctuations in the proneness to distraction. Previous neuroimaging studies found that the suppression of distracting inputs may be independent of the sampling of attended inputs[3,4,44]. Future investigations may manipulate both the target and distractor onset time to examine the

relationship between the temporal fluctuations underlying attentional sampling and distractibility.

Of note, as the main analysis approach used here (comparing empirical time courses to time courses that were shuffled in time) does not distinguish between periodic and aperiodic temporal structure[45], we are careful to conclude from the respective results alone that distractibility is rhythmic. However, it does not negate the possibility that there is a periodic temporal structure in distractibility. The premise of rhythmic cognition is that the apparent fluctuations of performance reflect the periodic orchestration between brain regions[12]. In addition to fluctuations in behavioural performance, neural evidence is therefore essential to elucidate the rhythmicity of cognition[46,47]. The current study shows a correspondence between slow neural oscillatory phase and behaviour (using an analysis approach that does not employ shuffling-in-time), consistent with the notion that distractibility is rhythmic. Future advancements in the analysis approach to directly test the periodicity in cognition will further strengthen our understanding of the distractibility dynamics.

Neural dynamics of distractibility originate in inferior frontal/insular cortices

The localisation of neural phase effects underlying distractibility dynamics beyond auditory cortex regions might suggest that the proneness to distraction is supra-modal. In research on visual distraction, brain regions in frontal and parietal cortices have been associated with distractor interference in lesions[27] or transcranial magnetic stimulation[28,29] studies. The functional connectivity between the left inferior frontal cortex and hippocampus is associated with the disruptive influence of task-irrelevant visual distraction on working memory[48]. While the current study examined distractibility in the auditory modality, the neural origins found here overlap with previous research on distraction in the visual modality.

The observed relationship between perceptual sensitivity and the inferior frontal/insular theta phase suggests that fluctuations in distractibility may be related to the cognitive control of working memory. The left inferior frontal cortex is assumed to be critical to the resolution of competition between the maintenance of goal-relevant information and the interference from external distraction[28,49,50]. The anterior insula is theorised as a gatekeeper to the brain regions responsible for goal-related cognitive control[51], and is part of the ventral attention system[52]. Specifically, the insular cortex may support the switching between networks important to internally directed and externally directed cognition, respectively[53]. The frontal theta rhythm

is associated with cognitive control[54–56] and the prioritization of relevant memory representation[57]. Taken together, theta oscillations in the inferior frontal and insular cortices may reflect the orchestration of the cognitive control system to maintain the internal memory representation and suppress potentially distracting external inputs.

Against what might have been expected, the pre-distractor neural phase did not predict fluctuations in the distractor-evoked neural response (Figure S8). However, this null result might rest on the distractor-evoked ERP being a rather unspecific proxy of distraction. Components of the distractor-evoked ERP have been shown to reflect cognitive operations other than distraction, such as reactive suppression[58–60] or stimulus prediction[61]. Distractibility dynamics may only account for a small amount of variance in the distractor-evoked ERP.

Conclusion

The present study demonstrates that human proneness to distraction is not uniformly distributed across time but fluctuates on a subsecond timescale in cycles of ~3 – 5 Hz. In the brain, time windows of higher distractibility are coined by stronger neural responses to distractors. Furthermore, slow neural phase in left inferior frontal/insular cortex regions explains fluctuations in distractibility. These results unravel the temporal dynamics of distractibility and thereby help explain human processing of an abundant kind of stimulus in increasingly complex environments, that is, irrelevant and distracting input.

References

1. Desimone, R. & Duncan, J. Neural mechanisms of selective visual attention. *Annual review of neuroscience* **18**, 193–222 (1995).

2. Picton, T. W., Hillyard, S. A., Galambos, R. & Schiff, M. Human auditory attention: a central or peripheral process? *Science* **173**, 351–353 (1971).

3. Schneider, D., Göddertz, A., Haase, H., Hickey, C. & Wascher, E. Hemispheric asymmetries in EEG alpha oscillations indicate active inhibition during attentional orienting within working memory. *Behavioural Brain Research* **359**, 38–46 (2018).

4. Wöstmann, M., Alavash, M. & Obleser, J. Alpha oscillations in the human brain implement distractor suppression independent of target selection. *J. Neurosci.* **39**, 9797–9805 (2019).

5. Wöstmann, M. *et al.* The vulnerability of working memory to distraction is rhythmic. *Neuropsychologia* **146**, 107505 (2020).

6. Bonnefond, M. & Jensen, O. Alpha oscillations serve to protect working memory maintenance against anticipated distracters. *Current Biology* **22**, 1969–1974 (2012).

7. Geng, J. J. & DiQuattro, N. E. Attentional capture by a perceptually salient non-target facilitates target processing through inhibition and rapid rejection. *Journal of Vision* **10**, 1–12 (2010).

8. van Moorselaar, D., Lampers, E., Cordesius, E. & Slagter, H. A. Neural mechanisms underlying expectation-dependent inhibition of distracting information. *eLife* **9**, e61048 (2020).

9. Weisz, N., Kraft, N. G. & Demarchi, G. Auditory cortical alpha/beta desynchronization prioritizes the representation of memory items during a retention period. *eLife* **9**, e55508 (2020).

10. Posner, M. I., Snyder, C. R. & Davidson, B. J. Attention and the detection of signals. *Journal of Experimental Psychology: General* **109**, 160–174 (1980).

11. Buschman, T. J. & Kastner, S. From Behavior to Neural Dynamics: An Integrated Theory of Attention. *Neuron* **88**, 127–144 (2015).

12. Fiebelkorn, I. C. & Kastner, S. A Rhythmic Theory of Attention. *Trends in Cognitive Sciences* **23**, 87–101 (2019).

13. Fiebelkorn, I. C., Saalmann, Y. B. & Kastner, S. Rhythmic Sampling within and between objects despite sustained attention at a cued location. *Current Biology* **23**, 2553–2558 (2013).

14. Ho, H. T., Leung, J., Burr, D. C., Alais, D. & Morrone, M. C. Auditory sensitivity and decision criteria oscillate at different frequencies separately for the two ears. *Current Biology* **27**, 3643-3649.e3 (2017).

15. Kubetschek, C. & Kayser, C. Delta/Theta band EEG activity shapes the rhythmic perceptual sampling of auditory scenes. *Scientific Reports* **11**, 2370 (2021).

16. Landau, A. N. & Fries, P. Attention samples stimuli rhythmically. *Current Biology* **22**, 1000–1004 (2012).

17. Schmid, R. R., Pomper, U. & Ansorge, U. Cyclic reactivation of distinct feature dimensions in human visual working memory. *Acta Psychologica* **226**, 103561 (2022).

18. ter Wal, M. *et al.* Theta rhythmicity governs human behavior and hippocampal signals during memory-dependent tasks. *Nat Commun* **12**, 7048 (2021).

19. Forster, S. & Lavie, N. Distracted by your mind? Individual differences in distractibility predict mind wandering. *Journal of Experimental Psychology: Learning, Memory, and Cognition* **40**, 251–260 (2014).

20. Campbell, K. L., Grady, C. L., Ng, C. & Hasher, L. Age differences in the frontoparietal cognitive control network: Implications for distractibility. *Neuropsychologia* **50**, 2212–2223 (2012).

21. Kannass, K. N., Oakes, L. M. & Shaddy, D. J. A longitudinal investigation of the development of attention and distractibility. *Journal of Cognition and Development* **7**, 381–409 (2006).

22. VanRullen, R. Perceptual Cycles. *Trends in Cognitive Sciences* **20**, 723–735 (2016).

23. Lakatos, P. *et al.* An Oscillatory Hierarchy Controlling Neuronal Excitability and Stimulus Processing in the Auditory Cortex. *Journal of Neurophysiology* **94**, 1904–1911 (2005).

24. Helfrich, R. F. *et al.* Neural mechanisms of sustained attention are rhythmic. *Neuron* **99**, 854-865.e5 (2018).

25. Rutishauser, U., Ross, I. B., Mamelak, A. N. & Schuman, E. M. Human memory strength is predicted by theta-frequency phase-locking of single neurons. *Nature* **464**, 903–907 (2010).

26. Siegel, M., Warden, M. R. & Miller, E. K. Phase-dependent neuronal coding of objects in short-term memory. *Proc. Natl. Acad. Sci. U.S.A.* **106**, 21341–21346 (2009).

27. Chao, L. & Knight, R. T. Human prefrontal lesions increase distractibility to irrelevant sensory inputs. *Neuroreport: An International Journal for the Rapid Communication of Research in Neuroscience* **6**, 1605–1610 (1995).

28. Wais, P. E., Kim, O. Y. & Gazzaley, A. Distractibility during episodic retrieval is exacerbated by perturbation of left ventrolateral prefrontal cortex. *Cerebral Cortex* **22**, 717–724 (2012).

29. Kanai, R., Dong, M. Y., Bahrami, B. & Rees, G. Distractibility in daily life Is reflected in the structure and function of human parietal cortex. *Journal of Neuroscience* **31**, 6620–6626 (2011).

30. Shamma, S. A., Elhilali, M. & Micheyl, C. Temporal coherence and attention in auditory scene analysis. *Trends in Neurosciences* **34**, 114–123 (2011).

31. Ding, N. & Simon, J. Z. Neural representations of complex temporal modulations in the human auditory cortex. *Journal of Neurophysiology* **102**, 2731–2743 (2009).

32. Wöstmann, M. *et al.* Ten simple rules to study distractor suppression. *Progress in Neurobiology* **213**, 102269 (2022).

33. Grabenhorst, M., Maloney, L. T., Poeppel, D. & Michalareas, G. Two sources of uncertainty independently modulate temporal expectancy. *Proc. Natl. Acad. Sci. U.S.A.* **118**, e2019342118 (2021).

34. Dürschmid, S. *et al.* Direct evidence for prediction signals in frontal cortex independent of prediction error. *Cerebral Cortex* 1–9 doi:10.1093/cercor/bhy331.

35. Herbst, S. K., Stefanics, G. & Obleser, J. Endogenous modulation of delta phase by expectation–A replication of Stefanics et al., 2010. *Cortex* **149**, 226–245 (2022).

36. Stefanics, G. *et al.* Phase entrainment of human delta oscillations can mediate the effects of expectation on reaction speed. *Journal of Neuroscience* **30**, 13578–13585 (2010).

37. Zoefel, B., Davis, M. H., Valente, G. & Riecke, L. How to test for phasic modulation of neural and behavioural responses. *NeuroImage* **202**, 116175 (2019).

38. Huang, Y., Chen, L. & Luo, H. Behavioral oscillation in priming: competing perceptual predictions conveyed in alternating theta-band rhythms. *Journal of Neuroscience* **35**, 2830–2837 (2015).

39. Schneider, D., Herbst, S. K., Klatt, L. & Wöstmann, M. Target enhancement or distractor suppression? Functionally distinct alpha oscillations form the basis of attention. *Eur J Neurosci* ejn.15309 (2021) doi:10.1111/ejn.15309.

40. Cruzat, J. *et al.* The phase of Theta oscillations modulates successful memory formation at encoding. *Neuropsychologia* **154**, 107775 (2021).

41. Geng, J. J. Attentional mechanisms of distractor suppression. *Curr Dir Psychol Sci* **23**, 147–153 (2014).

42. Dugué, L. & VanRullen, R. Transcranial magnetic stimulation reveals intrinsic perceptual and attentional rhythms. *Front. Neurosci.* **11**, (2017).

43. Lui, T. K.-Y. & Wöstmann, M. Effects of temporally regular versus irregular distractors on goal-directed cognition and behavior. *Scientific Reports* **12**, 10020 (2022).

44. Noonan, M. P. *et al.* Distinct mechanisms for distractor suppression and target facilitation. *J. Neurosci.* **36**, 1797–1807 (2016).

45. Brookshire, G. Putative rhythms in attentional switching can be explained by aperiodic temporal structure. *Nat Hum Behav* (2022) doi:10.1038/s41562-022-01364-0.

46. Fiebelkorn, I. C. Detecting attention-related rhythms: When is behavior not enough? (Commentary on van der Werf et al. 2021). *European Journal of Neuroscience* **55**, 3117–3120 (2022).

47. Wöstmann, M. Does attention follow a rhythm? *Nat Hum Behav* (2022) doi:10.1038/s41562-022-01365-z.

48. Wais, P. E., Rubens, M. T., Boccanfuso, J. & Gazzaley, A. Neural mechanisms underlying the impact of visual distraction on retrieval of long-term memory. *Journal of Neuroscience* **30**, 8541–8550 (2010).

49. Irlbacher, K., Kraft, A., Kehrer, S. & Brandt, S. A. Mechanisms and neuronal networks involved in reactive and proactive cognitive control of interference in working memory. *Neuroscience & Biobehavioral Reviews* **46**, 58–70 (2014).

50. Tops, M. & Boksem, M. A. S. A potential role of the inferior frontal gyrus and anterior insula in cognitive control, brain rhythms, and event-related potentials. *Front. Psychology* **2**, (2011).

51. Molnar-Szakacs, I. & Uddin, L. Q. Anterior insula as a gatekeeper of executive control. *Neuroscience & Biobehavioral Reviews* **139**, 104736 (2022).

52. Eckert, M. A. *et al.* At the heart of the ventral attention system: The right anterior insula. *Hum. Brain Mapp.* **30**, 2530–2541 (2009).

53. Uddin, L. Q. Salience processing and insular cortical function and dysfunction. *Nat Rev Neurosci* **16**, 55–61 (2015).

54. Berger, B. *et al.* Dynamic regulation of interregional cortical communication by slow brain oscillations during working memory. *Nat Commun* **10**, 4242 (2019).

55. Cavanagh, J. F. & Frank, M. J. Frontal theta as a mechanism for cognitive control. *Trends in Cognitive Sciences* **18**, 414–421 (2014).

56. Kamarajan, C. *et al.* The role of brain oscillations as functional correlates of cognitive systems: a study of frontal inhibitory control in alcoholism. *International Journal of Psychophysiology* **51**, 155–180 (2004).

57. Riddle, J., Scimeca, J. M., Cellier, D., Dhanani, S. & D'Esposito, M. Causal evidence for a role of theta and alpha oscillations in the control of working memory. *Current Biology* **30**, 1748-1754.e4 (2020).

58. Feldmann-Wüstefeld, T. & Vogel, E. K. Neural Evidence for the Contribution of Active Suppression During Working Memory Filtering. *Cerebral Cortex* **29**, 529–543 (2019).

59. Hickey, C., Di Lollo, V. & McDonald, J. J. Electrophysiological Indices of Target and Distractor Processing in Visual Search. *Journal of Cognitive Neuroscience* **21**, 760–775 (2009).

60. Wang, B., van Driel, J., Ort, E. & Theeuwes, J. Anticipatory Distractor Suppression Elicited by Statistical Regularities in Visual Search. *Journal of Cognitive Neuroscience* **31**, 1535–1548 (2019).

61. Volosin, M. & Horváth, J. Knowledge of sequence structure prevents auditory distraction: An ERP study. *International Journal of Psychophysiology* **92**, 93–98 (2014).

62. Oldfield, R. C. The assessment and analysis of handedness: The Edinburgh inventory. *Neuropsychologia* **9**, 97–113 (1971).

63. Brainard, D. H. The Psychophysics Toolbox. *Spatial Vision* **10**, 433–436 (1997).

64. Prins, N. & Kingdom, F. A. A. Applying the model-comparison approach to test specific research hypotheses in psychophysical research using the palamedes toolbox. *Front. Psychol.* **9**, 1250 (2018).

65. Macmillan, N. A. & Kaplan, H. L. Detection theory analysis of group data: Estimating sensitivity from average hit and false-alarm rates. *Psychological Bulletin* **98**, 185–199 (1985).

66. Oostenveld, R., Fries, P., Maris, E. & Schoffelen, J.-M. FieldTrip: open source software for advanced analysis of MEG, EEG, and invasive electrophysiological data. *Computational Intelligence and Neuroscience* **2011**, 156869 (2011).

67. Van Veen, B. D., Van Drongelen, W., Yuchtman, M. & Suzuki, A. Localization of brain electrical activity via linearly constrained minimum variance spatial filtering. *IEEE Trans. Biomed. Eng.* **44**, 867–880 (1997).

68. Maris, E. & Oostenveld, R. Nonparametric statistical testing of EEG- and MEG-data. *Journal of Neuroscience Methods* **164**, 177–190 (2007).

69. Koerner, T. K. & Zhang, Y. Effects of background noise on inter-trial phase coherence and auditory N1–P2 responses to speech stimuli. *Hearing Research* **328**, 113–119 (2015).

70. Mayhew, S. D., Dirckx, S. G., Niazy, R. K., Iannetti, G. D. & Wise, R. G. EEG signatures of auditory activity correlate with simultaneously recorded fMRI responses in humans. *NeuroImage* **49**, 849–864 (2010).

71. Oya, H. *et al.* Neural phase locking predicts BOLD response in human auditory cortex. *NeuroImage* **169**, 286–301 (2018).

Methods

Participants

Thirty participants (20 females, 10 males; mean age = 23.67, SD = 3.56) took part in the EEG experiment. They provided written informed consent and were compensated by either €10/hour or course credit. Participants were right-handed according to the Edinburgh Handedness Inventory[62] (mean score = 92), with self-reported normal hearing, normal or corrected-to-normal vision, and no psychological or neurological disorders. All procedures of the current study were approved by the ethics committee of the University of Lübeck.

Stimuli and Procedure

Participants performed a pitch discrimination task wherein they decided whether the first (tone 1) and the second (tone 2) target tones in a trial were the same or different in pitch. Prior to the experiment, they were instructed to answer as accurately and as fast as possible. The target tones were 75 ms long pure tones with 5 ms rise and fall periods. In each trial, the frequencies of tone 1 were randomly selected between musical note A#3 (233 Hz) and G#5 (830.6 Hz), while that of tone 2 was either the same (50%) or different (higher or lower, 25% each) in frequency compared to tone 1.

The pitch difference between tone 1 and tone 2 was titrated for each participant with an adaptive task (see below). The offset-to-onset interval between tone 1 and tone 2 was 1550 ms. Each distractor stimulus comprised 10 consecutive pure tones with 40 ms duration (400 ms in total). The frequencies of the pure tones in each distractor stimulus were randomly selected among the 12 tones between A#3 and G#5 with whole tone steps (A#3, C4, D4, E4, F#4, G#4, A#4, C5, D5, E5, F#5, and G#5), with the constraint that there would be no repetition between consecutive tones. Each of the 12 tone frequencies appeared at each of the 10 positions with equal probability across trials.

In-between the two target tones, a distractor was presented in 50% of trials (distractor-present condition) and no distractor was presented in the remaining trials (distractor-absent condition). In the distractor-present condition, the distractor was presented at one of 24 distractor onset times (0 ms to 1150 ms, 50-ms steps, relative to the offset of tone 1), which was selected at random on each trial. After the offset of target tone 2, participants had a 2000 ms response time window. To avoid potential temporal predictability effects of the onset of the

next trial, the inter-trial intervals were randomly selected from a truncated exponential distribution (mean = 1460 ms), ranging between 730 and 3270 ms.

The trial order was pseudo-randomized with no repetition in probe tone frequency and distractor onset for any two consecutive trials. In total, there were 12 trials for each unique condition (distractor-present/absent x distractor onset x same/different target pitch) and 1152 trials for the whole experiment. All auditory materials were presented via Sennheiser headphones (HD 25-1 II). Responses were made using a response box (The Black Box Toolkit). The assignment of buttons to the response options ("same" or "different") was counterbalanced across participants. Stimuli were presented via Matlab (MathWorks, Inc., Natick, USA) and Psychtoolbox[63]. The auditory stimuli were presented at approximately 70 dB SPL.

Adaptive Staircase Procedure

Prior to the main experiment, each participant's threshold for the pitch discrimination task was titrated using an adaptive staircase procedure, implemented in the Palamedes toolbox[64] for Matlab. For the initial 11 participants, the threshold was titrated to an approximate accuracy of 70.7%. As the overall accuracy was relatively high even after the adaptive staircase procedure for these 11 participants (mean = 79.59%, SD = 10.43%), the final 16 participants performed an adaptive procedure altered to yield approximately 65% accuracy instead. Due to technical issues, performance of the remaining three participants was tracked at 35% accuracy. As all relevant statistical analyses in the present study are within-subject, and as paired t-tests (2-tailed) comparing the behavioural performance between distractor-absent and distractor-present conditions were significant with ($t_{29} = 8.11$, $p < .001$) and without ($t_{26} = 9.41$, $p < .001$) these participants, their data were included in the final analysis.

Each participant went through the adaptive staircase procedure two to three times, depending on the stability of the tracked threshold. There were in total 30 trials for each run of the adaptive staircase procedure with an initial pitch difference of 100 cents (i.e. 1 semitone) between tone 1 and 2. The minimum and maximum pitch difference possible in the task was 2 cents and 2000 cents, respectively. For the procedure which tracked performance at ~70.7%, a two-down one-up procedure was used. Specifically, the pitch differences would decrease in steps of 10 cents if participant responded correctly (i.e., different), or increase in steps of 10 cents if participant responded incorrectly (i.e., same) for 2 consecutive trials. For the procedure which tracked performance at ~65% procedure, the pitch differences would decrease in steps

of 7 cents if participant answered correctly or increase in steps of 13 cents if they answered incorrectly. The pitch difference used in the main experiment was calculated by averaging the final 10 trials in the tracking run which converged to the most stable threshold, determined by visual inspection, in the ~70.7% procedure. The same procedure was used to average the final 6 trials in the ~65% procedure. Overall accuracy averaged across all participants in the actual experiment was 73.58% (SD = 12.12%).

Behavioural Data Analysis

To understand how distractors affect pitch discrimination performance in the framework of signal detection theory, we calculated sensitivity (d') and criterion (c) separately for distractor-present and -absent conditions, using the Palamedes toolbox[64] and the following formulas:

(Formula 1) Sensitivity = z (Hit rate) – z (False alarm rate)

(Formula 2) Criterion = –0.5 * (z (Hit rate) + z (False alarm rate))

Hit rate was defined as the "different" response when the two tones were different in pitch, and false alarm rate the "different" response when the two tones were the same in pitch. Extreme values (0 or 1) of Hit rate or False alarm rate were adjusted[65]: A rate of 0 was adjusted by dividing 1 by the number of trials multiplied by 2; while a value of 1 was adjusted by subtracting the same value from 1. Paired samples t-tests (2-tailed) were used to compare sensitivity and criterion in distractor-present versus -absent conditions.

To study the modulation of distractor onset times on behavioural measures in the distractor-present condition, sensitivity for each distractor onset time was calculated, resulting in a behavioural time course as a function of distractor onset time for each individual participant (see Fig. S1 & S2).

EEG Recording and Pre-processing

The experiment was conducted in an electrically shielded sound-attenuated room. A modified 10-20 international system with 64 Ag/Ag-Cl electrodes was used to record the EEG with a sampling rate of 1000 Hz (actiCHamp, Brain Products, München, Germany). The EEG recordings were band-pass filtered online from direct current (DC) to 280 Hz. TP9 was used as the online reference and FPz as the ground electrode. Impedances were kept below 20 kOhm for all but one participant.

Matlab R2018a (MathWorks, Inc., Natick, USA) and the Fieldtrip toolbox[66] were used to pre-process and analyse EEG data. The continuous EEG data were filtered (high-pass, 1 Hz; low-pass, 100 Hz) before they were segmented into epochs (-2 to 2.5s) time-locked to tone 1 onset. Independent component analysis (ICA) was used to identify and reject components corresponding to artefacts such as eye blinks, eye movements, and muscle activity (average percentage of components removed = 26.46%, SD = 8.89%). Afterwards, EEG data were re-referenced to the average of all electrodes. Epochs with amplitude changes >160 microvolts were rejected (average percentage of epochs removed = 1.35%, SD = 2%).

To obtain distractor-evoked neural responses, data were re-epoched to the onset of the distractor (-1 to 1 s) with a 200ms baseline period. Epochs belonging to the same conditions (distractor-present/absent) and distractor onset time (0 – 1150ms, 50-ms steps) were then averaged into ERP waveforms. The spectral amplitude of distractor-evoked responses at 25 Hz, which corresponds to the temporal structure of the distractor, was extracted using FFT on the ERP waveform in the time window from 0 to 520ms after distractor onset. Spectral amplitude was averaged across electrodes F1, Fz, F2, FC1, FCz, and FC2. For each participant, the 24 spectral amplitudes, corresponding to the 24 distractor onset times, resulted in a neural time course of distractor processing as a function of distractor onset time (see Fig. S1 & S2).

Distractor-evoked inter-trial phase coherence (ITPC) was also calculated across frequencies (1 – 10 Hz, 1-Hz steps) and time windows (-0.2 – 0.7 s, 0.05-s steps) for each electrode. First, Fourier coefficients were calculated (using windows with a fixed length of 0.5 s; hanning taper). Then, the complex Fourier coefficients were divided by their magnitude and averaged across trials. ITPC was calculated by taking the absolute value (i.e., magnitude) of the average complex coefficient.

Modulation of neural and behavioural measures by distractor onset time

To test whether and how distractor onset time modulates neural and behavioural measures, we used linear mixed-effect models with sine- and cosine-transformed distractor onset time, similar to Wöstmann et al. 2020[5]. For time courses of sensitivity and spectral amplitude of the distractor-evoked ERP at 25 Hz separately, we first subtracted the individually fitted quadratic trend (computed with the polyfit function in Matlab) from the original time course for each participant (see Fig. S1 & S2) as the quadratic trend was not of interest in the current study[38].

Then, we designed sine- and cosine- transformed distractor onset time vectors using the following formulas,

(Formula 3) Sine predictor = sin (2 * π * f * distractor onset time)

(Formula 4) Cosine predictor = cos (2 * π * f * distractor onset time)

Where f denotes the frequency of interest (0.5 – 8 Hz, 0.5-Hz steps). Next, we regressed the detrended sensitivity and spectral amplitude of ERP time courses on sine and cosine predictors using linear mixed models (using the fitlme function in Matlab) for each frequency of interest using the following formulas:

(Formula 5) z(sensitivity) ~ z(sine predictor) + z(cosine predictor) + (1|participant)

(Formula 6) z(25-Hz ERP) ~ z(sine predictor) + z(cosine predictor) + (1|participant)

Spectral magnitude for each frequency was computed by taking the square root of the sum of squared beta coefficients of sine and cosine predictors:

(Formula 7) Spectral magnitude = sqrt (sine $coef^2$ + cosine $coef^2$)

Statistical significance of the spectral magnitude was determined by comparing the spectral magnitude of the empirical data with the 95th percentile of a permutation distribution, which was generated by shuffling the original behavioural/neural time course and performing the same analysis for 5,000 times.

To test whether sensitivity and spectral amplitude of the distractor-evoked ERP at 25 Hz are co-modulated, for each participant, cross-correlation coefficients across time lags of the two signals were obtained (using the “xcorr” function on z-scored time courses in Matlab). Again, we ran a similar linear mixed model as explained above, but this time with sine- and cosine- transformed time lags as predictors and used the correlation coefficients from the cross-correlation as the outcome measure. Spectral magnitude was obtained using formula 7 and statistical significance with the same permutation method mentioned above.

Phasic modulation of behavioural sensitivity

To explore the role of pre-distractor neural dynamics on the pitch discrimination performance, we examined whether pre-distractor oscillatory phase relates to behavioural sensitivity. To this end, we examined the quadratic fit of sensitivity as a function of neural phase in source space.

First, we implemented the source analysis using the Fieldtrip toolbox. First, a standard volume conduction model and standard electrode locations were used to calculate the leadfield matrix with 10-mm resolution. We applied the linearly constrained minimum variance[67] (LCMV) beamformer approach on the 10 Hz lowpass filtered data centred around distractor onset (-1 to 1s). We calculated a common filter including all trials by calculating the covariance matrix estimates. There were in total 2,015 source locations inside the brain.

Second, a quadratic fit analysis resolved by frequency and time probed the spectral and temporal specificity of the phasic modulation of perceptual sensitivity. To obtain trial-wise phase values for each source location, the following procedure was implemented for each trial in each source location: First, the single-trial EEG time course was projected into the source space using the common filter. Then, a sliding window (0.4s duration; moving in 50-ms steps from –0.3 to +0.3s relative to distractor onset) was employed to transform the data into the frequency domain (using FFT). Note that the time point of the sliding window refers to the mid-point of each time window. For instance, the time window centred at -0.3 included data from -0.5 to -0.1 s. The respective phase value of each frequency (2.5 – 8 Hz in 0.5-Hz steps) was then calculated using the *angle* function in MATLAB. The phase values of all trials were binned into 9 bins of equal size, ranging from -pi to pi, followed by a calculation of sensitivity for each bin. The quadratic fit of sensitivity across phase bins was estimated using the *polyfit* function (order = 2) in MATLAB. As a result, we obtained a quadratic fit index for each source location, frequency, and time of interest.

We used a source-level cluster-based permutation test[68] to find significant clusters in voxel-frequency-time space that would exhibit phasic modulation of sensitivity. Dependent-samples t-tests were used to contrast quadratic fit coefficients against zero, followed by clustering of adjacent bins with significant effects in voxel-frequency-time space. To derive cluster p-values, summed t-values in observed clusters were tested against 5,000 permutations with shuffled condition labels (two-tailed).

To demonstrate that the significant cluster found in the above analysis does not primarily originate from auditory cortex, we localised, for comparison, the distractor-evoked inter-trial phase coherence (ITPC) at 3 – 7 Hz, strongly assumed to emerge at least to large degrees from the supratemporal plane and auditory cortex[69–71], with the following procedure for each voxel: For each trial, we projected the time series EEG data into source space using the same common filter as in the analysis on the phasic relationship with behaviour. Then, we transformed the source-projected data (0 – 300 ms after distractor onset) to the frequency domain using FFT. The same calculation as on the sensor level was used to calculate the ITPC for each frequency. ITPC across frequencies 3 – 7 Hz were then averaged to obtain one distractor-evoked ITPC value for each voxel.

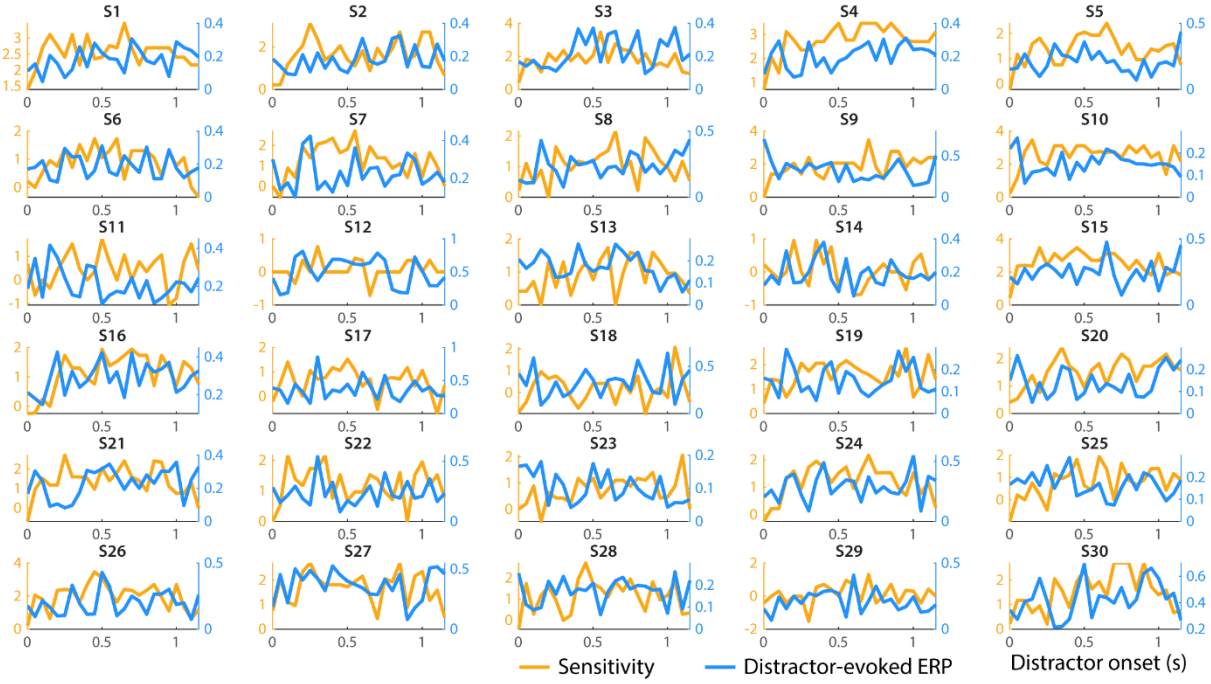

Figure S1. Time courses of raw sensitivity (yellow) and distractor-evoked ERP (25-Hz amplitude of distractor-evoked ERP; blue) for each individual participant.

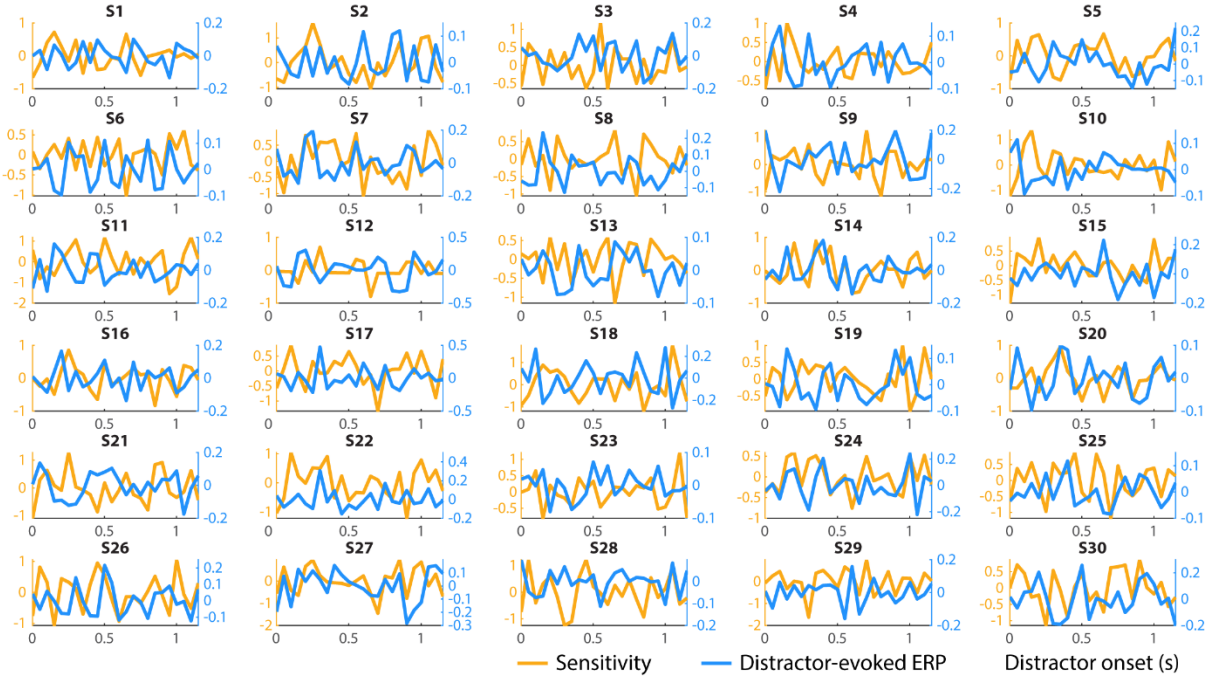

Figure S2. Detrended (quadratic trend removed) sensitivity (yellow) and distractor-evoked ERP (blue) time courses for each individual participant.

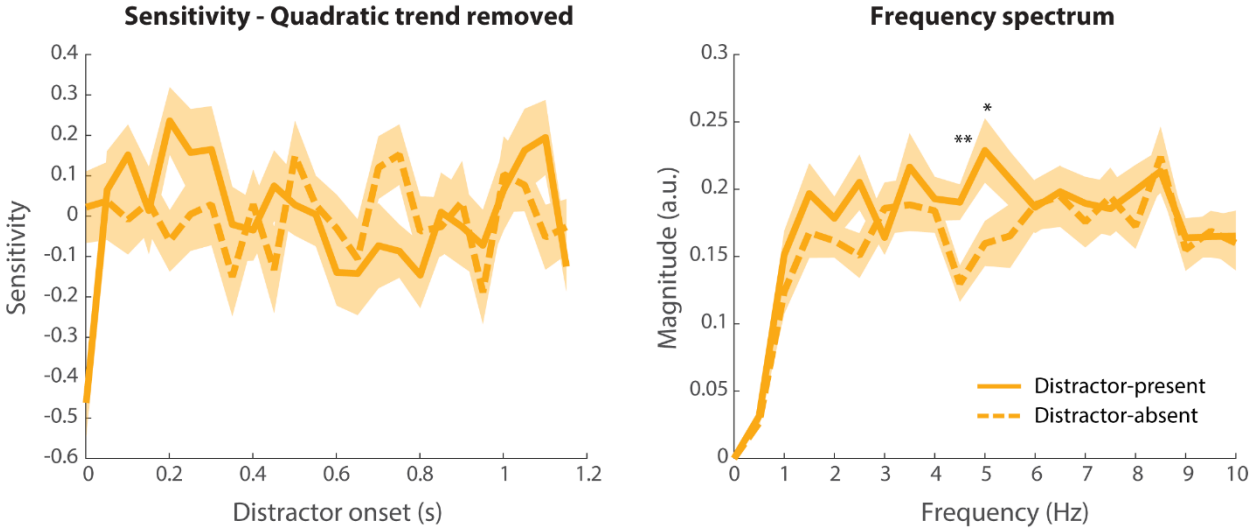

Figure S3. Left panel shows the sensitivity time courses for distractor-present (solid) and distractor-absent (dashed) conditions. Right panel shows the averaged frequency spectra, derived from FFT on single-subject time courses. Shaded areas show ±1 SEM across individual participants. Asterisks show statistical significance when comparing the spectral magnitude of distractor-present versus -absent conditions (using uncorrected dependent-samples t-tests). * $p < .05$ ** $p < .01$

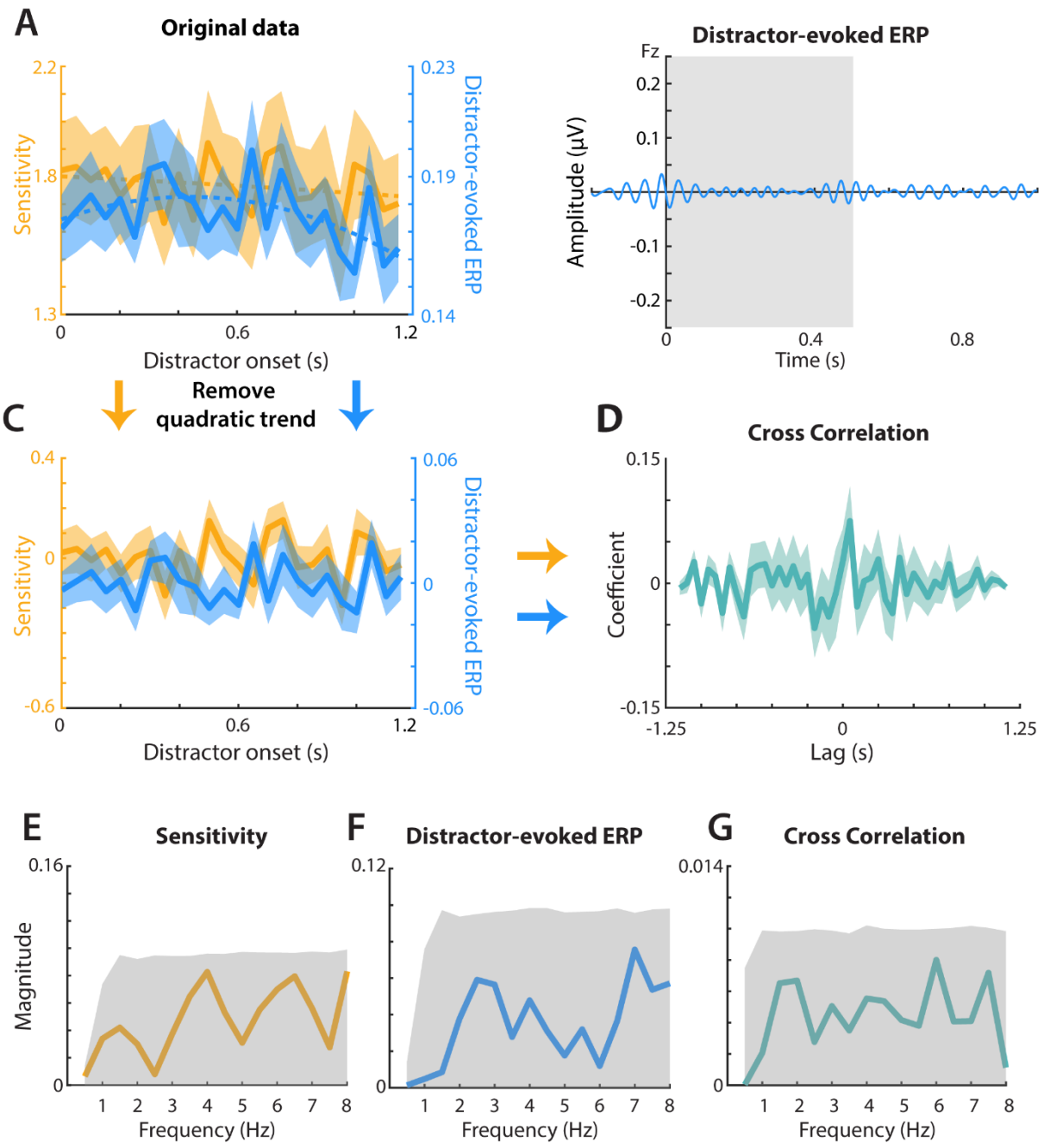

Figure S4. The same analysis pipeline as shown in Figure 2, applied here to the distractor-absent condition.

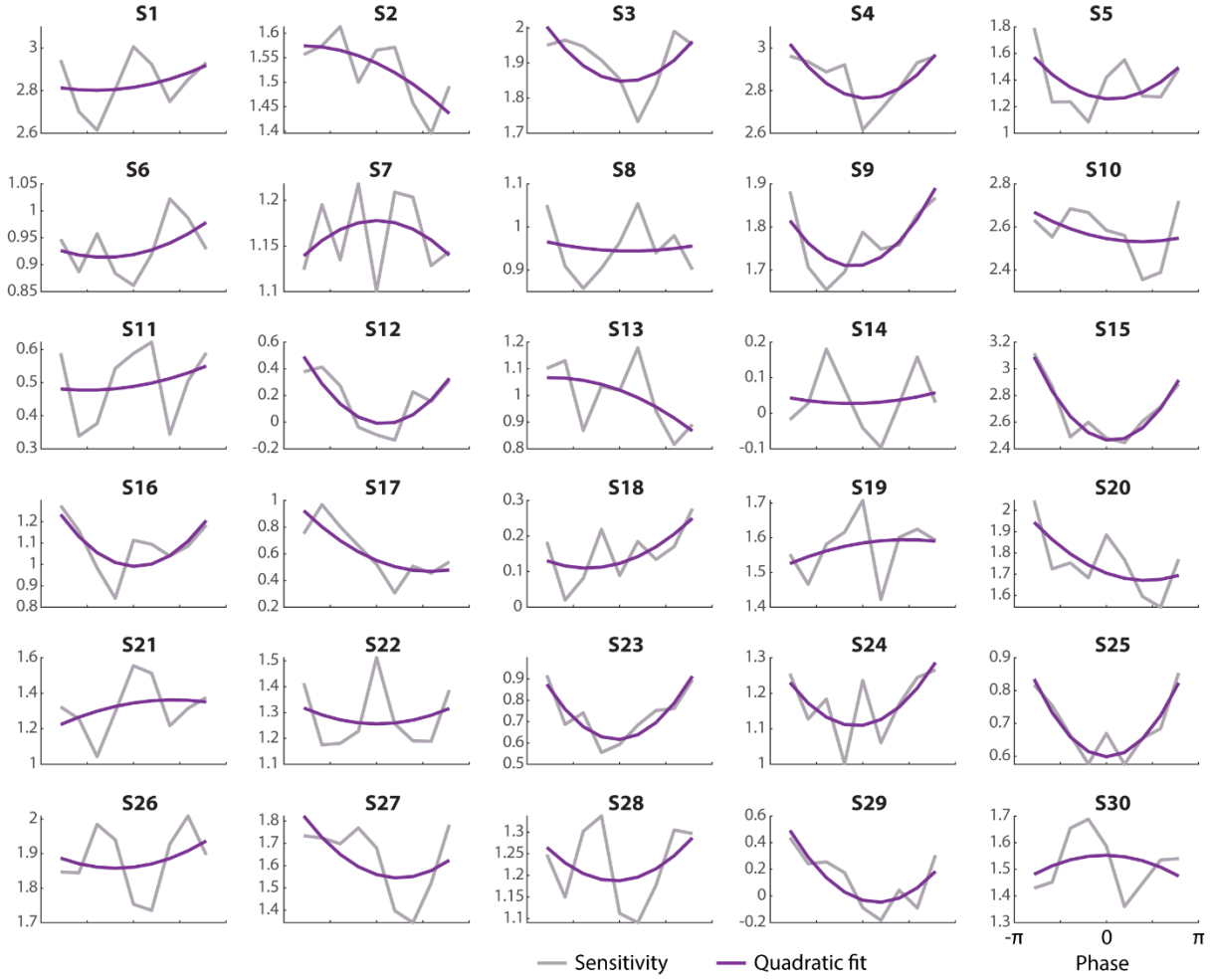

Figure S5. Individual sensitivity (grey line) and quadratic fit (purple line) across phase bins of the significant positive cluster at 3 Hz.

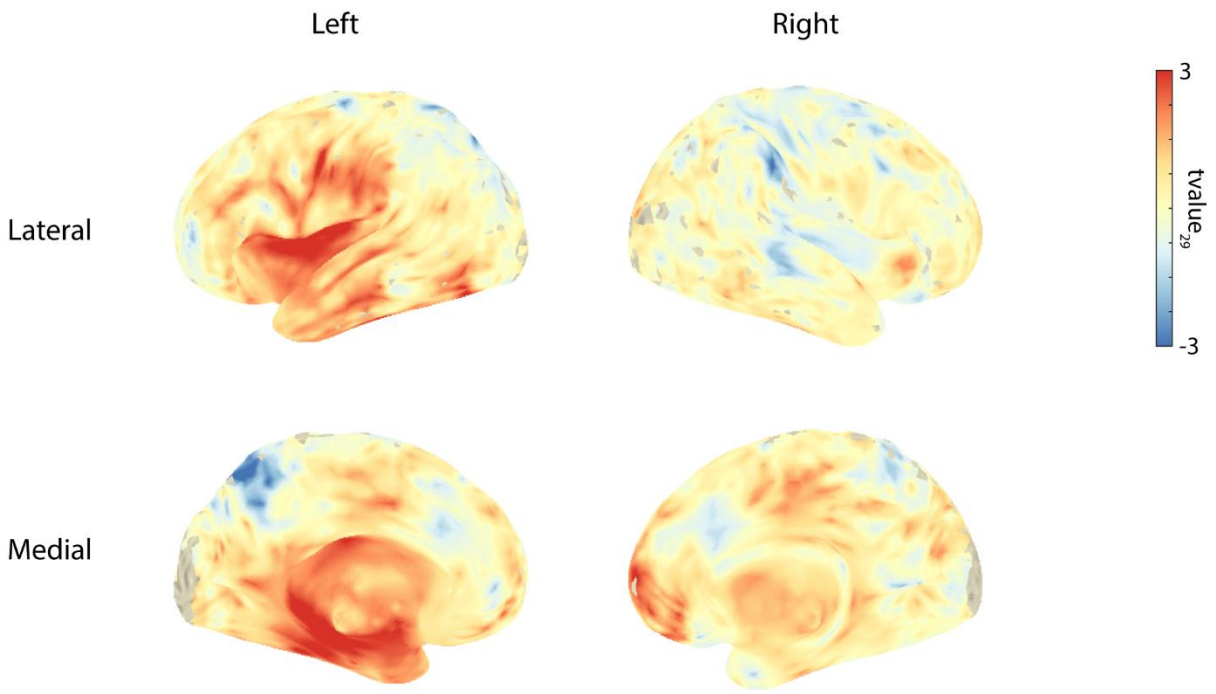

Figure S6. Brain surface plots of the cluster peak effect (3 Hz; -0.2 s) from left lateral (top left), right lateral (top right), left medial (bottom left), and right medial (bottom right) views show t-values for the comparison of the quadratic fit of the sensitivity sorted by phase bins against zero. The t-values were interpolated and projected onto MNI coordinates for visualization purposes.

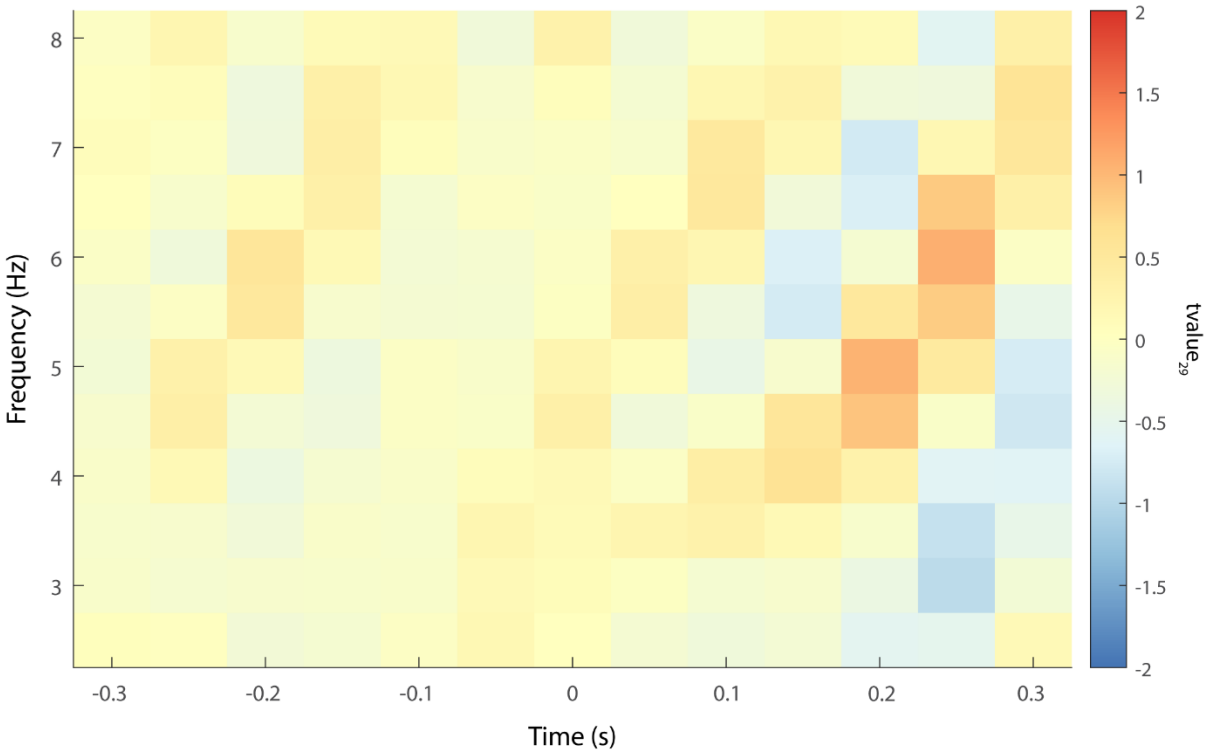

Figure S7. Results of the cluster-based permutation test, across time windows and frequencies, on the quadratic relationship between neural phase and sensitivity for the distractor-absent condition. Figure shows t-values (df = 29) averaged across all the voxels belonging to the significant positive cluster in the distractor-present condition shown in Figure 3. No significant cluster was found in the distractor-absent condition.

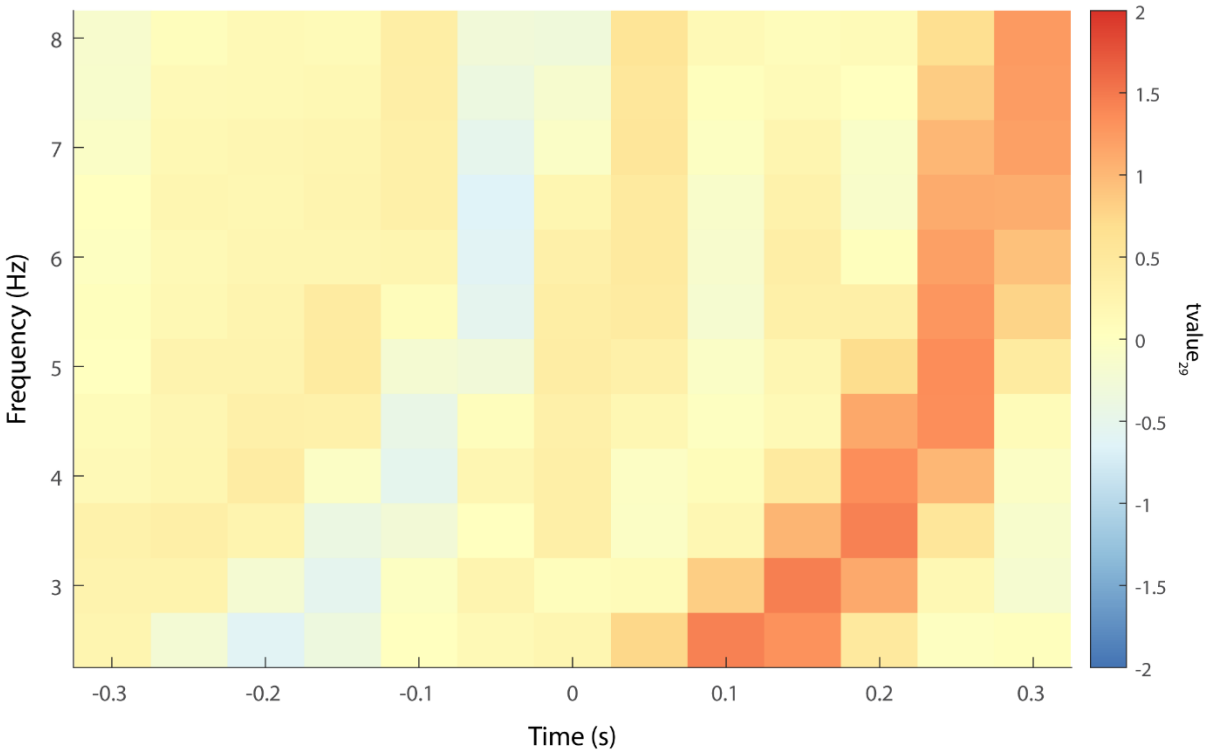

Figure S8. Results of the cluster-based permutation test, across time windows and frequencies, on the quadratic relationship between neural phase and distractor-evoked ERP amplitude at 25 Hz. Figure shows t-values (df = 29) averaged across all the voxels belonging to the significant positive cluster testing the quadratic relationship between neural phase and behavioural sensitivity shown in Figure 3. As expected, and not of main interest in the current study, a significant cluster in the post-stimulus time window (i.e., >0s) was found. More importantly, no significant cluster was found in the pre-distractor time window (i.e., <0 s).